IEEE Access
Multidisciplinary | Rapid Review | Open Access Journal

Received April 13, 2021, accepted May 16, 2021, date of publication May 24, 2021, date of current version June 7, 2021.

Digital Object Identifier 10.1109/ACCESS.2021.3083095

Performance Analysis of URLL Energy-Harvesting Cognitive-Radio IoT Networks With Short Packet and Diversity Transmissions

MOHAMMAD REZA AMINI[1], (Senior Member, IEEE), AND MOHAMMED W. BAIDAS[2], (Senior Member, IEEE)

[1]Department of Electrical Engineering, Islamic Azad University, Borujerd Branch, Borujerd 73916-9867, Iran
[2]Department of Electrical Engineering, College of Engineering and Petroleum, Kuwait University, Kuwait City 13060, Kuwait

Corresponding author: Mohammed W. Baidas (m.baidas@ku.edu.kw)

This work was supported in part by the Kuwait Foundation for the Advancement of Sciences (KFAS) under Project PN17-15EE-02.

ABSTRACT The advent of the Internet-of-Things (IoT) and proliferation of wireless devices and systems have put stringent requirements on reliability and latency, in addition to the scarcity of energy and spectrum resources. More importantly, ultra-reliability and low-latency (URLL) combined with concepts of energy-harvesting (EH) and cognitive-radio (CR) make the analysis of IoT networks much more complex. This paper analyzes the performance of uplink EH-CR-IoT networks with URLL requirements. Analytical expressions for IoT network metrics, namely, average packet latency, reliability, and energy-efficiency are derived, while incorporating diversity transmissions under the finite blocklength (FBL) regime. The effect of network parameters, such as number of resource blocks allocated to each IoT user equipment (UE), blocklength, and number of packet replicas is examined on the network metrics, and their tradeoffs are discussed. Finally, the derived expressions are utilized to maximize the energy-efficiency of the IoT UEs subject to energy-causality and URLL constraints.

INDEX TERMS Cognitive-radio, energy-harvesting, finite blocklength, Internet-of-Things, low-latency, ultra-reliability.

I. INTRODUCTION

The Internet-of-Things (IoT) has emerged as a promising networking paradigm for connecting massive numbers of smart systems and devices, which urgently call for spectrum- and energy-efficient transmission techniques to meet the diverse requirements of latency, reliability and energy-efficiency. Specifically, ultra-reliable and low-latency (URLL) transmissions are considered to be the main features for many IoT applications, such as factory automation, smart cities, tactile Internet, and industrial IoT [1]–[3]. To improve spectrum-efficiency, cognitive-radio (CR) has been put forth as a key solution to exploit under-utilized spectrum bands [4]. For energy-efficient transmissions under the green communications paradigm, energy-harvesting (EH) technologies have emerged as viable solutions to alleviate the need to replace/recharge batteries or rely on the electrical grid, and thus help meet the energy demands of wireless devices and networks [5]. On the other hand, URLL communication (URLLC) can be achieved via several techniques. Specifically, ultra-reliability can be realized by diversity transmission, in which multiple replicas of a packet are sent to the destination. To achieve low-latency, short packet transmissions via finite blocklength (FBL) codes can be employed [6]. The analysis of EH-CR-IoT networks with URLL requirements is of paramount importance for 5G and beyond cellular networks, and hence, is the focus of this paper.

A. RELATED WORKS

To date, several studies have focused on achieving URLLC in cellular networks, which is challenging due to the interplay between various operational parameters and transmission schemes [7], [8]. For instance, for a factory automation scenario with non-orthogonal multiple-access (NOMA), the authors in [9] jointly optimized the blocklength and power allocation to minimize the decoding error probability of the actuator, subject to the reliability requirement of the relay robot. It has been shown that the relay-assisted transmission significantly outperforms its OMA counterpart.

The associate editor coordinating the review of this manuscript and approving it for publication was Javed Iqbal.

A cross-layer optimization for URLLC in radio access networks is given in [10], where the packet dropping, power allocation, and bandwidth allocation policies have been optimized to minimize the transmit power under the URLL constraints. In [11], a novel availability maximization resource allocation scheme for coordinated multi-point (CoMP) transmission with URLLC provisioning is proposed, and demonstrated to achieve the highest availability in comparison to existing schemes. A characterization of different design parameters to support downlink (DL) URLLC in OFDMA-based 5G wireless networks is considered in [12]. Specifically, the authors study the impact of system bandwidth, link signal-to-interference-plus-noise ratio (SINR), quality-of-service (QoS) parameters, and hybrid automatic repeat request (HARQ) on the URLLC capacity, and highlight the different performance tradeoffs. A graph-theoretical approach in smart factory scenario with successive interference calculation to achieve URLLC for IoT applications is proposed in [13], and shown to improve spectral-efficiency without degrading the fairness. Centralized low-complexity multi-cell scheduling algorithms are devised in [14], with results showing up to 60% latency improvement over existing distributed scheduling schemes. In [15], the energy-latency tradeoff in URLLC systems is studied, while employing incremental redundance (IR) and HARQ. In particular, a dynamic programming algorithm is devised for IR-HARQ optimization in terms of blocklength, power per round, and number of retransmissions, which is shown to achieve around 25% energy saving in comparison to the one-shot transmission (i.e. no HARQ). Other works have considered resource allocation, network slicing, link adaptation, and scheduling for enhanced mobile broadband (eMBB) with URLLC requirements [16]–[18]. Our previous works [19], [20] analyzed the performance of random-access NOMA (RA-NOMA) with clustered IoT devices in URLL-EH-IoT networks, where analytical expressions for network metrics–such as average packet latency, reliability, and GoodPut—are derived. More importantly, the RA-NOMA scenario has been compared to its RA-OMA counterpart to illustrate the merits of NOMA over OMA.

However, only few researchers have studied URLL communications in spectrum sharing and CR networks. For example, an adaptive channel assignment method—based on machine-learning along with fountain codes—is proposed in [21] to reduce transmission latency, and ensure reliability in licensed and unlicensed spectrum bands. Particularly, the authors proposed switching the critical data to the licensed spectrum with the best channel conditions, and the non-critical data to the least congested unlicensed spectrum. Opportunistic spectrum access in underlay CR networks to achieve URLLC has been analyzed in [22]. By adopting an ARQ scheme for secondary transmissions, the maximum achievable rate, the approximate rate at high signal-to-noise ratios (SNRs), and the optimal secondary user average transmit power under statistical received power outage constraint have been achieved. Note that none of aforementioned CR studies employed short packet transmissions in their models. Table 1 provides a summary of the aforementioned studies.

B. MOTIVATION AND CONTRIBUTIONS

As stated earlier, IoT networks with massive numbers of IoT nodes and URLL requirements entail spectrum- and energy-efficient transmission strategies, making the combination of CR and EH inevitable. Although a few studies have focused on URLLC in spectrum sharing scenarios, to the best of our knowledge, no study considered URLLC in CR-IoT networks with EH nodes. In turn, this paper focuses on the analysis of uplink EH-CR-IoT networks with URLL requirements. Specifically, the IoT user equipments (UEs) are assumed to have non-saturated data traffic, and transmit their data packets in the FBL regime via RA spectrum sharing.

TABLE 1. Summary of different studies on URLLC with FBL.

Ref.	Network Model and Scenario	Objective
[9]	Downlink NOMA/OMA in factory automation	Optimization of blocklength and power allocation for decoding error probability minimization
[10]	OFDMA-based radio access networks with spatial diversity	Cross-layer optimization framework for resource allocation and packet dropping policies to minimize transmit power
[11]	Coordinated multi-point transmission in 5G networks	Optimization of blocklength and SINR to maximize resource availability
[12]	OFDMA-based 5G networks with HARQ	Study the impact of system bandwidth, SINR, and HARQ
[13]	IoT in a dense smart factory	Exploiting a graph-theoretical approach to improve spectral-efficiency
[14]	5G centralized multi-cell radio access networks with HARQ	Adopting centralized multi-cell scheduling algorithms for latency improvement
[15]	Point-to-point communication with IR and HARQ	Adopting dynamic programming to optimize blocklength, power per round, and number of retransmissions for average energy minimization
[19]	Clustered uplink RA-NOMA IoT network with EH nodes	Performance analysis and optimization of transmit power, number of replicas, and number of transmitted data bits per blocklength for GoodPut maximization
[20]	Clustered uplink RA-NOMA IoT networks	Performance analysis and exploration of the effect of number of replicas, and number of data bits per blocklength on network metrics
[21]	Spectrum sharing in licensed and unlicensed mmWave bands	Adopting a machine learning approach and fountain codes for adaptive channel assignment to reduce transmission latency, and ensure reliability
[22]	Spectrum sharing in underlay CR networks with ARQ	Optimization of SU average transmit power under outage constraint for achievable rate maximization

Short-length packets with diversity transmission are adopted to satisfy the URLL requirements. Furthermore, multiple resource blocks (RBs) can be selected by the IoT UEs in each TTI to transmit multiple data packets simultaneously in a frame, leading to further reduction in packet latency. Also, the average packet latency, reliability and energy-efficiency of the IoT UEs are analytically derived. In deriving the reliability, collisions among the IoT UEs as well as channel decoding errors due to exploiting the FBL codes are considered. Transmission delay and buffer waiting time are accounted for in deriving the average packet latency. Thus, the main contributions of this paper are summarized as follows:

- An URLL EH-CR-IoT network is studied, where transmission diversity in the FBL regime is exploited to meet the stringent target reliability and latency.
- Analytical expressions for the average packet latency, reliability, and energy-efficiency are derived. To this aim, the distribution of the IoT UEs transmission process is derived. Then, the analytical expressions of the network metrics are obtained by employing the $z-$operator and queueing theory, while accounting for the collisions between IoT UEs due to the dynamic spectrum access, and channel decoding errors due to employing short-length packets.
- The effect of the number of RBs allocated to each IoT UE, blocklength, and transmission diversity on the average packet latency, reliability, and energy-efficiency is investigated. Then, the tradeoff between reliability and average packet latency resulting from varying the number of idle RBs, packet replicas, and blocklength is highlighted and discussed. Moreover, the feasible and infeasible regions for fulfilling the packet latency and reliability constraints for different numbers of packet replicas and blocklengths are determined, providing more insights for IoT applications and requirements.
- The IoT UEs energy-efficiency maximization problem subject to energy-causality and URLL constraints on the average packet latency and reliability is solved by utilizing the derived analytical expressions. Specifically, the blocklength as well as the number of packet replicas and required RBs are optimized for energy-efficiency maximization.

It is worth-mentioning that this study is different from our URLLC-based previous works in [19], [20]. Specifically, this work considers a different network model that brings dynamic spectrum access (i.e. cognitive radio) with energy-harvesting nodes into the IoT paradigm, while [19], [20] analyze network metrics in uplink RA-NOMA IoT networks with URLL requirements. The IoT UEs in this study are assumed to access the spectrum dynamically through spectrum sharing with primary users. This makes the network analysis fundamentally different, since the random behavior of the primary users and their data traffic pattern greatly influence the transmission process of the IoT UEs. Furthermore, to lower the packet queueing delay, this work assumes that each IoT UE is able to select a number of RBs to simultaneously transmit multiple packets in one transmission time interval (TTI), as opposed to the randomly selected RB by clustered IoT UEs in [19], [20]. Additionally, the multi-user nature of the problem in hand, and the IoT UEs' interaction are prominent differences that affect the different IoT network metrics.

The rest of this paper is organized as follows. Section II introduces the system model. The analytical derivations of the different IoT network metrics are given in Section III. The numerical results are presented in Section IV. In Section V, the energy-efficiency maximization problem is formulated and solved. Future research directions of this work are outlined in Section VI. Finally, conclusions are drawn in Section VII.

II. SYSTEM MODEL

A. IoT NETWORK MODEL

Consider an uplink CR-IoT network with N IoT UEs that scavenge environmental energy (e.g. solar and/or wind) to cater for their transmissions to the base-station (BS). The IoT UEs exploit the spectrum shared with a cellular primary network,[1] as shown in Fig. 1.

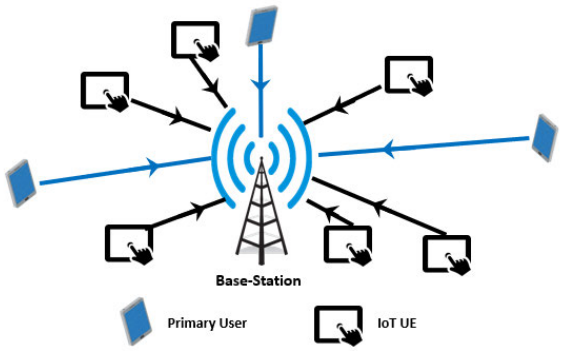

FIGURE 1. IoT network model.

All UEs schedule their transmissions in a time-slotted fashion, where each time-slot or TTI is called a *frame*[2] [25]–[27]. Each frame is of duration of T_f, and consists of R orthogonal RBs, each of bandwidth B. To avoid collisions with the primary UEs, the BS provides the information of vacant RBs on a reference broadcasting channel [28]. At the beginning of each frame, if there exist at least p idle RBs (for $p \in \{1, \ldots, R\}$), each IoT UE having at least p data packets in its buffer starts transmitting its data packets over the p idle RBs, which are randomly selected among all idle RBs determined by the BS on the reference channel. If the number of idle RBs is less than p, then the IoT UEs must wait for the next frame to find an adequate number of idle RBs. Thus, each IoT UE buffers p of its data packets for transmission over p RBs (i.e. one packet per RB). Note that selecting multiple RBs allows the IoT UEs to send several packets in a single

[1]There are many existing scenarios (e.g. industrial IoT) in which an IoT network coexists with a licensed cellular network [23]–[25].

[2]In this paper, the terms "TTI" and "frame" are used interchangeably.

frame, which in turn lowers the number of in-queue packets, and decreases the packet's waiting time, ultimately reducing the packet transmission latency.

Remark 1: The traffic behavior of each IoT UE for the generated data packets follows a Poisson arrival process with arrival rate of λ_d.[3]

To achieve ultra-reliability in such a multi-channel multi-user scenario, diversity transmission is adopted, where each data packet is sent multiple times (say $\mathcal{K}$ times) in successive TTIs. Therefore, the packet loss rate is reduced at the expense of transmission redundancy. Furthermore, short packet transmission is adopted to realize low-latency transmissions [6], [8]. However, in such a case, the Shannon's capacity is no longer applicable, as the decoding error due to employing the FBL regime is non-negligible. In turn, for transmissions with a blocklength of $n_b > 100$ and n_d data bits per packet, the decoding error probability is approximated as [31]

$$P_\epsilon \approx Q\left(\sqrt{\frac{n_b}{V(\gamma)}}\left(C(\gamma) - \frac{n_d}{n_b}\right)\right) \triangleq \Upsilon(\gamma, n_b, n_d), \quad (1)$$

where γ is the received SNR at the BS, $C(\gamma) = \log_2(1+\gamma)$ is the Shannon capacity, $V(\gamma) = (1 - \frac{1}{1+\gamma^2})(\log_2 e)^2$ is the channel dispersion, and $Q(\cdot)$ is the Q-function, as given by $Q(x) = \frac{1}{\sqrt{2\pi}}\int_x^\infty e^{-u^2/2}$. The channel coefficient between the i^{th} IoT UE and the BS is denoted h_i.[4] Therefore, the corresponding channel gain $|h_i|^2$ follows an exponential distribution with mean $d_i^{-\nu}$, where d_i is the corresponding distance, while ν is the path-loss exponent. Furthermore, the background noise over all links is assumed to be independent and identically distributed (i.i.d.) zero-mean additive white Gaussian noise with variance $\sigma^2 = BN_0$, where N_0 is the noise spectral density. It should be noted that γ is stochastic, and hence, the average decoding error probability can be determined as

$$\overline{\Upsilon}(\gamma, n_b, n_d) = \int_0^\infty \Upsilon(\gamma, n_b, n_d) f_\gamma(\theta) d\theta, \quad (2)$$

where $f_\gamma(\theta)$ is the probability density function (PDF) of γ.

B. PRIMARY NETWORK MODEL

The primary network is assumed to be cellular, which is the case in many IoT applications. Moreover, the traffic behavior of the primary UE (PUE) is modeled as a two-state continuous-time Markov chain (CTMC) with idle and busy rates of λ_0 and λ_1, respectively.[5] The stationary probability of idle and busy states are obtained as $\Pi_0 = \frac{\lambda_1}{\lambda_1+\lambda_0}$ and $\Pi_1 = \frac{\lambda_0}{\lambda_1+\lambda_0}$, respectively [35].

[3]This model has been widely used in communication networks [29], [30].

[4]All the channels in the network experience independent but not necessarily identically distributed (i.n.n.i.d.) Rayleigh block fading. Moreover, the channel gains remain constant within each transmission block but vary independently between different blocks.

[5]This is the most common traffic model used for primary networks [32]–[34], where the state idle (busy) implies the absence (presence) of the PUE.

C. ENERGY MODEL

The energy is assumed to arrive randomly in each frame as quantized energy packets. To model its randomness, the harvested energy arrival process $\mathcal{E}^h$ at each frame m (for $m = 0, 1, \ldots$) is modeled as an i.i.d. stationary random process with rate λ_e [36]–[39]. In turn, the expected value of the harvested energy during a frame is $\mathbb{E}\left[\mathcal{E}^h\right] = \lambda_e T_f$, where $\mathbb{E}[\cdot]$ is the expectation operator. The harvested energy is then stored in a rechargeable battery with infinite capacity. Moreover, let $\mathbb{P}_t$ be the IoT UE's transmit power, and $\mathbb{P}_c$ be circuitry power consumption when the IoT UE waits for the next frame to find an adequate number of idle RBs.

To analyze the EH-CR-IoT network, some of the main parameters should be described. Table 2 summarizes the main symbols used in this study and their descriptions.

TABLE 2. Notations.

Symbol	Description
γ	Received SNR at BS
π_i	Steady-state probability of the TTI being of type $\mathcal{T}_i$
B	Bandwidth of each RB
$\mathbb{P}_t$	Transmission power
$\mathbb{P}_c$	Circuitry power consumption
n_b	Blocklength
n_d	Number of data bits in a packet
λ_0	Stationary probability of the channel being idle
λ_1	Stationary probability of the channel being busy
N	Number of IoT UEs
T_f	Frame duration
T_D	Packet transmission delay
T_C	Transmission cycle
T_L	Transmission latency
p	Number of selected idle RBs in a frame for data transmission
R	Total number of RBs in a frame
$\mathcal{K}$	Number of replicas for each data packet
λ_d	Data packet arrival rate for the IoT node
λ_e	Energy arrival rate for the IoT node
d_i	Distance of i^{th} IoT UE to BS
ν	Path-loss exponent

III. DERIVATIONS OF NETWORK METRICS

In this section, the analytical derivations of different network metrics are presented. However, a few definitions must first be given.

Definition 1 (Packet Transmission Delay): A packet transmission delay T_D is the time duration during which a typical packet is transmitted by an IoT UE. Specifically, T_D is a random variable referring to the time needed to transmit a typical packet when it is ready.

Definition 2 (Transmission Cycle): A transmission cycle T_C is the time duration in which a typical data packet and all its replicas are transmitted by an IoT UE of interest.[6] Accordingly, T_C is a random variable taking the minimum

[6]Note that T_D and T_C incorporate all the frames in which the underlying IoT UE waits due to not finding at least p idle RBs.

value of $\mathcal{K} \times T_f$ seconds if the IoT UE finds at least p idle RBs for all $\mathcal{K}$ successive frames.

Definition 3 (Packet Latency): The packet latency T_L is the total delay that a typical data packet and all its replicas incur to be received at BS, which includes the transmission cycle and waiting time in the buffer.

Definition 4 (Energy-Efficiency): Energy-Efficiency η_e is defined as the average effective redundancy-free (i.e. non-repeated) received bits at the BS per unit time per unit energy (i.e. in bits/s/Joule).

Definition 5 (Reliability): Reliability $\mathcal{R}$ is defined as the probability that a transmitted data packet is received successfully at the BS (i.e. without any collision and/or channel decoding error).

Definition 6 (TTI Type): The following TTI types are defined in the network:

TTI type i $(\mathcal{T}_\mathbf{i})$:
A TTI at the beginning of which there exist i data packets (for $i = 1, 2, \ldots, p-1$) in the IoT UE's buffer. From a steady-state perspective, a typical TTI is of type $\mathcal{T}_\mathbf{i}$ with probability of π_i.[7]

TTI type p_+ $(\mathcal{T}_{\mathbf{p}_+})$:
A TTI at the beginning of which there exist at least p data packets in the buffer of the IoT UE. From the steady-state perspective, a typical frame is of type $\mathcal{T}_{\mathbf{p}_+}$ with probability of π_{p_+}.

A. PACKET TRANSMISSION DELAY DISTRIBUTION

The PDF of the transmission delay T_D for an IoT UE's packet, $f_{T_D}(t)$, is obtained in **Lemma 1**. In deriving such a distribution, all the TTIs that an IoT UE has to wait to find sufficient number of idle RBs are considered.

Lemma 1: The PDF of the IoT UE's packet transmission delay is obtained as

$$f_{T_D}(t) = \sum_{j=1}^{\infty} \left(\mathcal{P}_{p_-}\right)^{j-1} \left(1 - \mathcal{P}_{p_-}\right) \delta(t - jT_f), \tag{3}$$

where $\delta(.)$ is the Dirac delta function, and $\mathcal{P}_{p_-}$ is given by

$$\mathcal{P}_{p_-} = \sum_{i=0}^{p-1} \binom{R}{i} \Pi_0^i \left(1 - \Pi_0\right)^{R-i}. \tag{4}$$

Proof: See Appendix A. ∎

B. TRANSMISSION CYCLE DISTRIBUTION

According to the definition of the transmission cycle T_C, it consists of successive attempts for transmitting $\mathcal{K}$ replicas of a typical packet. **Lemma 2** gives the expression for the transmission cycle and its expected value.

Lemma 2: The PDF of the IoT UE's packet transmission cycle T_C is obtained as

$$f_{T_C}(t) = \sum_{l=\mathcal{K}}^{\infty} \binom{l-1}{\mathcal{K}-1} \left(1 - \mathcal{P}_{p_-}\right)^{\mathcal{K}} \left(\mathcal{P}_{p_-}\right)^{l-\mathcal{K}} \delta\left(t - lT_f\right). \tag{5}$$

[7]This probability is derived in subsection III-C.

Furthermore, the expected value of T_C (i.e. $\mathbb{E}\left[T_C\right] \triangleq \mu_{T_C}$) is obtained as

$$\mu_{T_C} = \frac{\mathcal{K} T_f}{1 - \mathcal{P}_{p_-}}. \tag{6}$$

Proof: See Appendix B. ∎

C. AVERAGE PACKET LATENCY

To derive the expected value of packet latency, one must first obtain the average packet waiting time in an IoT UE buffer. To this aim, the steady-state probabilities π_i (for $i = 0, 1, \cdots$) of the TTI types must be derived. Such probabilities are derived according to **Lemmas 3** and **4**. In **Lemma 3**, a recursive equation is presented to derive π_i for $i = p, p+1, \cdots$. Then, the p initial probabilities π_i (for $i = 0, 1, \ldots, p-1$) are derived in **Lemma 4** based on the recursive equation obtained in **Lemma 3**.

Lemma 3: The steady-state probabilities π_{j+p} (for $j = 0, 1, \cdots$) are obtained recursively via

$$\pi_{j+p} = \frac{1}{a_0} \left(\pi_j - a_j \bar{\pi}_p - \sum_{i=p}^{j+p-1} \pi_i a_{j+p-i} \right), \tag{7}$$

where $\bar{\pi}_p \triangleq \sum_{i=0}^{p-1} \pi_i$. Furthermore, a_i (for $i = 0, 1, \ldots$) is determined as

$$a_i = \frac{\left(T_f \lambda_d\right)^i}{i!} \left(\frac{1 - \mathcal{P}_{p_-}}{\mathcal{P}_{p_-}} \right)^{\mathcal{K}} \sum_{l=\mathcal{K}}^{\infty} \binom{l-1}{\mathcal{K}-1} l^i \left(\mathcal{P}_{p_-} e^{-T_f \lambda_d} \right)^l. \tag{8}$$

Proof: See Appendix C. ∎

Lemma 4: The first p steady-state probabilities π_i (for $i = 0, 1, \ldots, p-1$) are determined by solving the following set of equations

$$p(1 - \bar{\pi}_p) = \Psi - \sum_{i=0}^{p-1} i \pi_i, \tag{9a}$$

$$\bar{\pi}_p - z_l^{-p} \sum_{i=0}^{p-1} \pi_i z_l^i = 0, \quad \text{for } l = 1, \ldots, p, \tag{9b}$$

where $\Psi \triangleq \frac{\mathcal{K} \lambda_d T_f}{1 - \mathcal{P}_{p_-}}$. Furthermore, z_l (for $l = 1, \ldots, p$) are the zeros of $z^p = \left(\frac{(1 - \mathcal{P}_{p_-}) e^{\lambda_d (z-1) T_f}}{1 - \mathcal{P}_{p_-} e^{\lambda_d (z-1) T_f}} \right)^{\mathcal{K}}$.

Proof: See Appendix D. ∎

Now, the average packet latency of the underlying EH-CR-IoT network is obtained via **Lemma 5**.

Lemma 5: The average packet latency (i.e. $\mathbb{E}[T_L] \triangleq \mu_{T_L}$) in an IoT UE's buffer is derived as per (10) as shown at the bottom of the next page.

Proof: See Appendix E. ∎

D. RELIABILITY

The reliability $\mathcal{R}$ of a typical IoT UE is defined as the probability of successfully transferring a data packet to the BS, which is determined as given in **Lemma 6**.

Lemma 6: The IoT UE's reliability is derived as

$$\mathcal{R} = 1 - (P_e)^{\mathcal{K}}, \tag{11}$$

where P_e is obtained as

$$P_e = 1 - P(E_{NDE})\, P(E_{NC}). \tag{12}$$

Particularly, $P(E_{NDE}) = 1 - \overline{\Upsilon}(\gamma, n_b, n_d)$ is the probability of no decoding error (NDE) due to channel distortion, and $P(E_{NC})$ is the probability of no collision (NC) among the UEs over the selected RBs, as given by (13) as shown at the bottom of the page.

Proof: See Appendix F. ■

E. ENERGY-EFFICIENCY

The energy-efficiency η_e of the IoT UE is defined as ratio of the average effective rate of an IoT UE to the average amount of consumed energy in a typical transmission cycle, and is obtained as per **Lemma 7**.

Lemma 7: The energy-efficiency for a typical IoT UE η_e is determined as

$$\eta_e = \frac{\left(1 - \mathcal{P}_{p_-}\right)^2 p \mathcal{R} n_d}{\mathcal{K}^2 T_f \left[\mathbb{P}_t T_f (1 - \mathcal{P}_{p_-}) + \mathbb{P}_c T_f \mathcal{P}_{p_-}\right]}. \tag{14}$$

Proof: See Appendix G. ■

F. ENERGY-CAUSALITY

Energy-causality is an important constraint in EH networks, which ensures that the average consumed energy $\mathcal{E}^c$ cannot exceed that of the harvested. Mathematically, such a constraint can be written for a typical frame, say m^{th} frame, as $\mathbb{E}[\mathcal{E}_m^c] \leq \mathbb{E}[\mathcal{E}_m^h]$. From a steady-state perspective, the energy-causality constraint is obtained in **Lemma 8**.

Lemma 8: The energy-causality constraint for each IoT UE is given as

$$\left(1 - \bar{\pi}_p\right)\left((\mathbb{P}_c - \mathbb{P}_t)\mathcal{P}_{p_-} + \mathbb{P}_t\right) T_f \leq \lambda_e T_f. \tag{15}$$

Proof: See Appendix H. ■

IV. NUMERICAL RESULTS

In this section, the effect of the number of packet replicas $\mathcal{K}$, blocklength n_b, and the number of RBs allocated to each IoT UE on the average packet latency, reliability, and energy-efficiency is evaluated. The simulated network parameters are set according to Table 3 unless stated otherwise [40].

TABLE 3. Simulation parameters.

Parameter	Value	Parameter	Value
N	50	R	30 RBs
n_d	50	$(\mathbb{P}_t, \mathbb{P}_c)$	(0.2, 0.05) W
λ_e	0.2 J/s	λ_d	1000s^{-1}
λ_0	0.1s^{-1}	λ_1	0.2s^{-1}
ν	3	B	100 KHz
d_i	0.7 Km	N_0	-174 dBm/Hz

Fig. 2 illustrates the effect of $\mathcal{K}$ and n_b on the average packet latency μ_{T_L}. As can be seen, μ_{T_L} increases with the increase in $\mathcal{K}$ and n_b. This is because increasing the number of packet replicas increases the transmission cycle of each individual packet, leading to an increase in μ_{T_L}. On the other hand, the frame duration is increased by increasing n_b, resulting in further increase in μ_{T_L}.

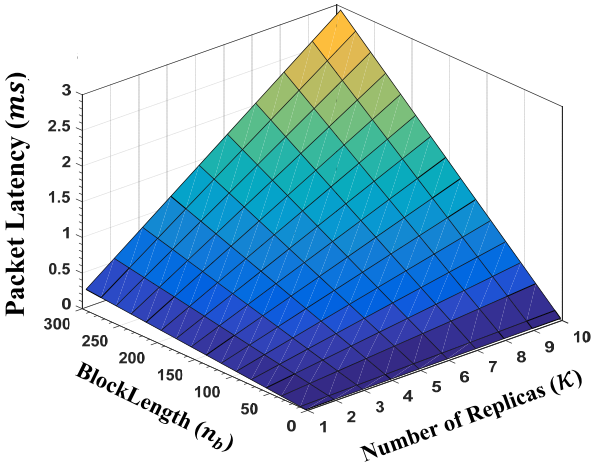

FIGURE 2. Average packet latency vs. $\mathcal{K}$ and n_b – $p = 10$.

In Fig. 3, the IoT UE's reliability as a function of $\mathcal{K}$ and n_b is demonstrated. Clearly, $\mathcal{R}$ improves when the number of packet replicas increases, since higher orders of diversity transmission result in increased successfully received packets. Furthermore, the higher the number of blocklength bits is, the less the decoding error probability, and hence, the higher the reliability. It is worth-mentioning that there is a tradeoff between the reliability and average packet latency, as increasing both $\mathcal{K}$ and n_b exacerbates the average packet latency but improves the reliability. To meet the stringent URLL requirements in the IoT applications of the emerging Industry

$$\mu_{T_L} = \frac{\mathcal{K} T_f}{1 - \mathcal{P}_{p^-}} + \frac{\Psi^2(\mathcal{K} + \mathcal{P}_{p^-}) + 2\mathcal{K}\Psi\left[p(\bar{\pi}_p - 1) - \sum_{i=0}^{p-1} i\pi_i\right] + \mathcal{K}p\,(1+p)\,(1-\bar{\pi}_p) - \mathcal{K}\sum_{i=0}^{p-1} i\,(i-1)\,\pi_i + 2\mathcal{K}p\sum_{i=0}^{p-1} i\pi_i}{2\mathcal{K}\lambda_p(p - \Psi)} \tag{10}$$

$$P(E_{NC}) = \sum_{j=1}^{N-1}\sum_{l=2p}^{R}\left(\frac{\binom{l-p}{p}(1-\bar{\pi}_p)}{\binom{l}{p}}\right)^j \binom{R}{l}\Pi_0^l(1-\Pi_0)^{R-l} + \sum_{l=p}^{R}\binom{R}{l}\Pi_0^l(1-\Pi_0)^{R-l} \tag{13}$$

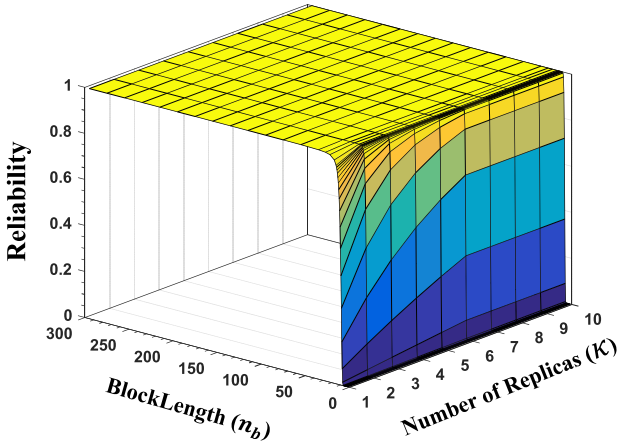

FIGURE 3. Reliability vs. $\mathcal{K}$ and $n_b - p = 10$.

4.0 paradigm,[8] $\mathcal{K}$ and n_b must be set appropriately. To this aim, Fig. 4 is plotted, where the green area satisfies both the reliability and packet latency requirements for $p = 10$.

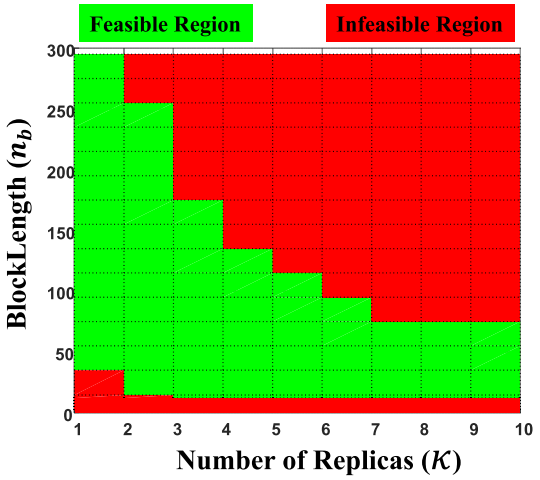

FIGURE 4. Feasible and infeasible regions of satisfying the average packet latency and reliability constraints - $p = 10$.

Fig. 5 depicts the energy-efficiency η_e versus $\mathcal{K}$ and n_b. Evidently, transmitting higher number of packet replicas yields significant reduction in η_e. This is because the higher the number of packet replicas is, the longer the transmission cycle. Thus, the number of effective data bits transmitted per time unit decreases. Moreover, increasing $\mathcal{K}$ leads to an increase in energy consumption. This explains the severe decrease in η_e observed in Fig. 5. Another observation is that for extremely low values of n_b, η_e is also low, which is due to the excessively high decoding error at the BS. Moreover, slightly increasing n_b leads to higher number of successfully decoded data bits (or equivalently lower decoding error), which improves η_e. However, excessively increasing n_b lowers η_e. This is because the excessive increase in n_b does not yield further improvement in the decoding error. On the contrary, it increases the frame duration and transmission cycle,

[8]Example applications include motion control and factory automation with latency and reliability of 1 ms and 99.999%, respectively [41], [42].

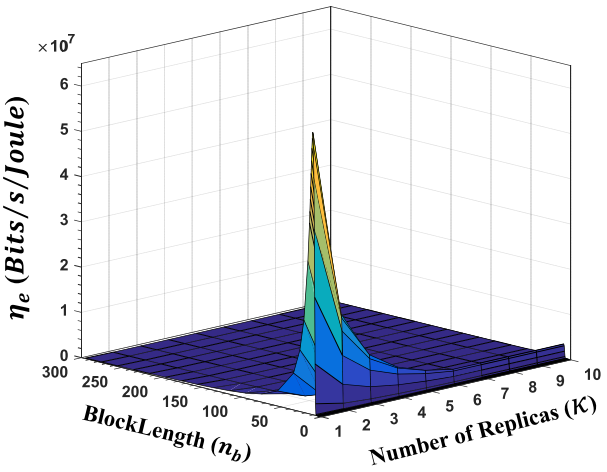

FIGURE 5. Energy-efficiency vs. $\mathcal{K}$ and $n_b - p = 10$.

which increases the consumed energy, leading to a significant decrease in the number of effective data bits transmitted per time and energy units.

The average packet latency μ_{T_L} as a function of the number of packet replicas $\mathcal{K}$ and idle RBs p is depicted in Fig. 6. In alignment with the observation made for $\mathcal{K}$ in Fig. 2, one can see that when more packet replicas are transmitted, the transmission cycle increases, leading to an increase in μ_{T_L}. Furthermore, higher μ_{T_L} is observed when the number of idle RBs is very low. This is because the lower the number of idle RBs to be selected by the IoT UE in a frame, the higher the number of data packets in the IoT UEs buffer, and thus, the longer the in-buffer waiting time and the higher the average packet latency. Additionally, μ_{T_L} also increases when the number of employed RBs in a frame p is high. This is due to the fact that the IoT UE must wait longer to find a higher number of idle RBs in a frame. Hence, a typical data packet experiences further delay in waiting for a frame with adequate number of idle RBs.

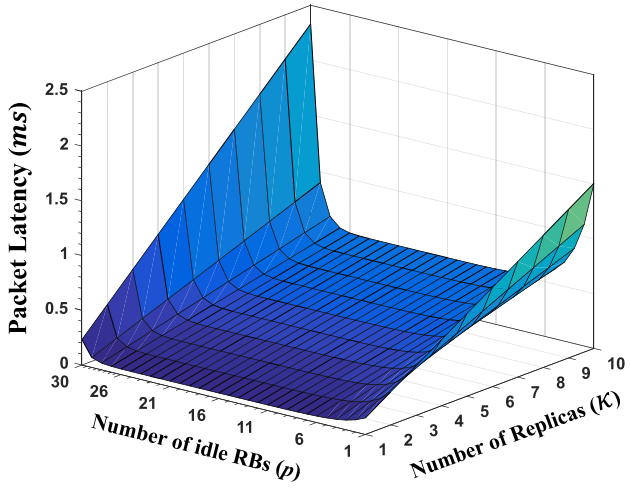

FIGURE 6. Average packet latency vs. $\mathcal{K}$ and $p - n_b = 30$.

Fig. 7 depicts the IoT UE reliability versus $\mathcal{K}$ and p. As can be seen, the reliability increases with the increase in $\mathcal{K}$, as the

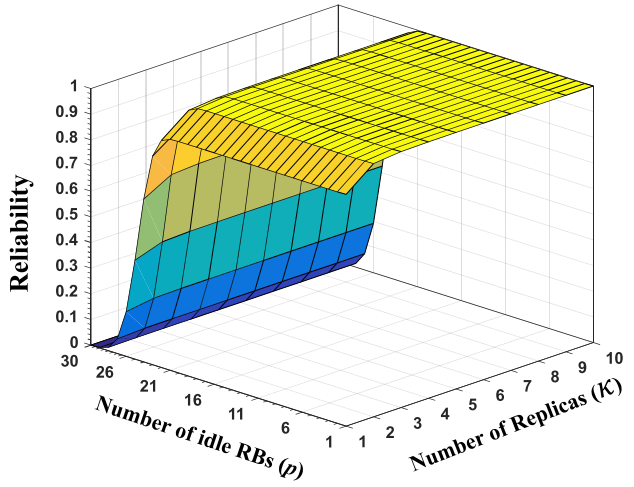

FIGURE 7. Reliability vs. $\mathcal{K}$ and $p - n_b = 30$.

higher the number of packet replicas is, the higher the number of successfully delivered packets. However, it is observed that the reliability decreases by increasing p. This is because the higher the number of RBs to be selected by the IoT UEs in a frame, the higher the probability of collision among them, and hence, the lower the reliability.

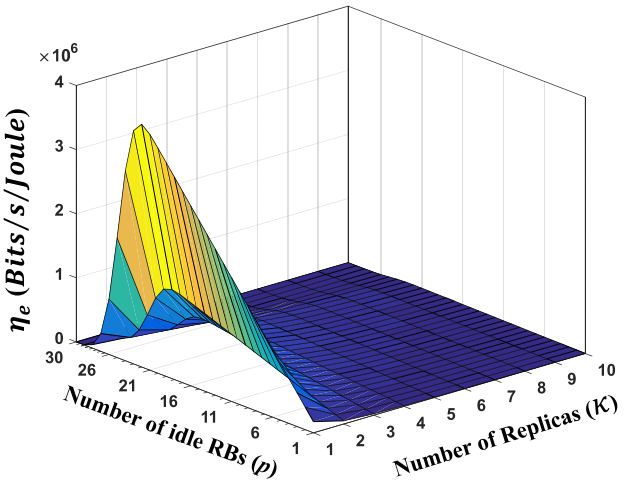

FIGURE 8. Energy-Efficiency vs. $\mathcal{K}$ and $p - n_b = 30$.

The effect of $\mathcal{K}$ and p on the energy-efficiency η_e is investigated in Fig. 8. Evidently, the higher the number of packet replicas is, the longer the transmission cycle and the higher the consumed energy. This reduces the effective transmitted data bits per time and energy units, and therefore, reduces the energy-efficiency. On the other hand, η_e experiences low values when p is low. This is because the effective transmitted data bits in a frame is low when the number of selected idle RBs p is low. This explains why increasing p results in higher values of η_e, as can be seen in Fig. 8. However, when the IoT UEs are allowed to select higher numbers of idle RBs in a frame, the collision between the IoT UEs increases. This in turn reduces the effective transferred data bits per time unit, ultimately lowering the energy-efficiency.

V. ENERGY-EFFICIENCY MAXIMIZATION

The analytical derivations of the different network metrics can be utilized to optimize the energy-efficiency of the IoT UEs, subject to constraints on energy-causality, average packet latency, and reliability. Specifically, the energy-efficiency maximization (EE-MAX) problem can be formulated as

EE-MAX:

$$\max_{n_b,\mathcal{K},p} \ \eta_e \tag{16a}$$

$$\text{s.t } (1-\bar{\pi}_p)\Big((\mathbb{P}_c-\mathbb{P}_t)\mathcal{P}_{p_-}+\mathbb{P}_t\Big)T_f \leq \lambda_e T_f \tag{16b}$$

$$\mu_{T_L} \leq \delta_{th}^{L} \tag{16c}$$

$$\mathcal{R} \geq \delta_{th}^{R} \tag{16d}$$

$$n_b, \mathcal{K}, p \in \{1, 2, \ldots\}. \tag{16e}$$

In problem **EE-MAX**, Constraint (16b) enforces energy-causality, while Constraint (16c) ensures that the maximum average packet latency does not exceed δ_{th}^{L}. Moreover, Constraint (16d) is the reliability requirement, which is at least δ_{th}^{R}. The last constraint defines the range of values the decision variables take. Notably, the optimal values n_b, K and p can achieve the stringent URLL requirements for IoT applications, as per 3GPP and ITU specifications [43], [44].

Remark 2: Problem **EE-MAX** is a nonlinear integer programming problem, which is non-convex and computationally-intensive [45]. This is evident from the nonlinear analytical expressions of η_e, μ_{T_L}, and $\mathcal{R}$, and the integer-valued decision variables. Despite the non-convexity of problem **EE-MAX**, the incurred computational delay is irrelevant, which is due to the steady-state analysis.[9]

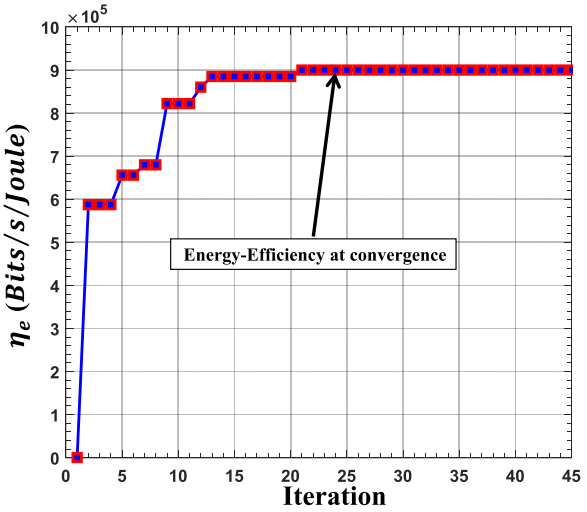

FIGURE 9. Convergence to optimal solution for energy-efficiency.

Fig. 9 illustrates the number of iterations required to achieve the EE optimal solution. The optimal objective function value is 9×10^5 bits/s/Joule, while the optimal values of the decision variables are $(n_b, \mathcal{K}, p) = (32, 3, 14)$ when

[9]Problem **EE-MAX** is solved via the global optimization package MIDACO [46], [47], with tolerance set to 10^{-6}.

$\delta_{th}^{R} = 0.99999$, and $\delta_{th}^{L} = 1$ms. Also, the optimal EE value is determined in less than 21 iterations, and thus, the optimal solution can be determined efficiently.

VI. FUTURE RESEARCH DIRECTIONS

To guarantee QoS in URLLC, reliability and packet latency requirements must be fulfilled throughout the communication network. Due to the non-stationary environment, model mismatch, and the existence of uncertainty in practical communication systems, theoretical analyses and QoS performance indicators derived based on system models have to be integrated into learning approaches to achieve accurate configurations and network settings. In turn, several studies have incorporated artificial intelligence approaches to fine-tune network settings and transmission policies [48]. Hence, the theoretical results can be used to initially train deep neural networks (DNNs), and quantify the network's performance limits [49]. Furthermore, the theoretical analyses and derived analytical expressions can be used as a labeled training data set for off-line training to further fine-tune DNNs in non-stationary scenarios, and subsequently be used to initialize DNNs for online implementations. Additionally, deep transfer learning (DTL) can be used to overcome the model mismatch problem with the aid of appropriate training samples in new environments. As another potential research direction, one can derive theoretical results for different data arrival rates, and then use it along with traffic predictions to devise transmission policies [50].

VII. CONCLUSION

In this paper, an uplink EH-CR-IoT network with URLL requirements has been analyzed. Particularly, the EH IoT UEs—characterized with non-saturated data traffic—aim at accessing the shared spectrum randomly. The IoT network metrics, namely, average packet latency, reliability, and energy-efficiency have been analyzed, while incorporating short packet and diversity transmissions. To reduce the average packet latency, multiple resource blocks can selected by the IoT UEs in a frame to send multiple data packets simultaneously. In turn, the effect of number of packet replicas, idle resource blocks, and blocklength, and their tradeoffs are investigated on the network metrics. Particularly, to improve the reliability, both the number of replicas and the blocklength should be increased; however, at the expense of the average packet latency. Furthermore, higher values of the average packet latency are observed when either the number of idle RBs is very low or very high. It is also observed that the reliability decreases with the increase in the number of selected idle RBs. Additionally, energy-efficiency is degraded when the number of packet replicas increases. It also experiences low values when the number of selected idle RBs is very low or very high. Such an effect is seen when varying the blocklength. In turn, the network parameters must be carefully chosen to meet the URLL requirements. Lastly, the derived expressions have been utilized to maximize the energy-efficiency, subject to energy-causality and URLL constraints.

APPENDIX A
PROOF OF LEMMA 1

Proof: To derive the PDF of the packet transmission delay, note that the transmission delay of a typical packet is determined by the number of TTIs that the IoT UE spends on finding the required number of idle RBs (i.e. p RBs). Notably, if the IoT UE finds at least p idle RBs in the first TTI, then the transmission delay equals T_f. In general, if the IoT UE finds less than p idle RBs in $j-1$ consecutive TTIs, and then finds at least p idle RBs in the j^{th} TTI, then the transmission delay is equivalent to $j \times T_f$. Hence, $f_{T_D}(t)$ is written as

$$f_{T_D}(t) = \sum_{j=1}^{\infty} \left(\mathcal{P}_{p_-}\right)^{j-1} \left(1 - \mathcal{P}_{p_-}\right) \delta(t - jT_f), \tag{A.1}$$

in which $\delta(.)$ is the Dirac delta function. Moreover, $\mathcal{P}_{p_-}$ denotes the probability that the IoT UE finds less than p idle RBs in a typical TTI, and thus can be found as

$$\mathcal{P}_{p_-} = \sum_{i=0}^{p-1} \binom{R}{i} \Pi_0^i \left(1 - \Pi_0\right)^{R-i}. \tag{A.2}$$

■

APPENDIX B
PROOF OF LEMMA 2

Proof: To derive the PDF of the packet transmission cycle, note that a transmission cycle can be expressed as the sum of $\mathcal{K}$ independent packet transmission delays (i.e. $T_C = \sum_{i=1}^{\mathcal{K}} T_{D_i}$). To derive the distribution of T_C, its characteristic function $\Phi_{T_C}(\omega)$ is determined as

$$\Phi_{T_C}(\omega) = \mathbb{E}\left[e^{jT_C\omega}\right] = \mathbb{E}\left[e^{j\omega\sum_{i=1}^{\mathcal{K}} T_{D_i}}\right]. \tag{B.1}$$

Since all T_{D_i}'s are independent of each other, then

$$\begin{aligned}
\Phi_{T_C}(\omega) &= \mathbb{E}\left[\prod_{i=1}^{\mathcal{K}} e^{j\omega T_{D_i}}\right] = \prod_{i=1}^{\mathcal{K}} \mathbb{E}\left[e^{j\omega T_{D_i}}\right] \\
&= \prod_{i=1}^{\mathcal{K}} \int_0^{\infty} e^{j\omega t_i} f_{T_D}(t_i) dt_i \\
&= \prod_{i=1}^{\mathcal{K}} \left(\sum_{l=1}^{\infty} \left(\mathcal{P}_{p_-}\right)^{l-1} \left(1 - \mathcal{P}_{p_-}\right) \int_0^{\infty} e^{j\omega t_i} \delta(t_i - lT_f) dt_i \right) \\
&= \prod_{i=1}^{\mathcal{K}} \left(\sum_{l=1}^{\infty} \left(\mathcal{P}_{p_-}\right)^{l-1} \left(1 - \mathcal{P}_{p_-}\right) e^{j\omega l T_f} \right).
\end{aligned} \tag{B.2}$$

By applying the geometric series formulae, $\Phi_{T_C}(\omega)$ is obtained as

$$\Phi_{T_C}(\omega) = \prod_{i=1}^{\mathcal{K}} \frac{\left(1 - \mathcal{P}_{p_-}\right) e^{j\omega T_f}}{1 - \mathcal{P}_{p_-} e^{j\omega T_f}} = \left(\frac{\left(1 - \mathcal{P}_{p_-}\right) e^{j\omega T_f}}{1 - \mathcal{P}_{p_-} e^{j\omega T_f}} \right)^{\mathcal{K}}. \tag{B.3}$$

It can be verified that the obtained characteristic function is that of the negative binomial random variable [51]. Hence, considering that T_C is the sum of several TTIs (i.e. $T_C \in \{\mathcal{K}T_f, (\mathcal{K}+1)T_f, \ldots\}$), its PDF can be presented as

$$f_{T_C}(t)=\sum_{l=\mathcal{K}}^{\infty}\binom{l-1}{\mathcal{K}-1}\left(1-\mathcal{P}_{p_-}\right)^{\mathcal{K}}\left(\mathcal{P}_{p_-}\right)^{l-\mathcal{K}}\delta(t-lT_f). \quad \text{(B.4)}$$

The expected value of the transmission cycle can be easily derived by the property of characteristic function as

$$\mathbb{E}\left[T_C\right]=\frac{d}{jdw}\Phi_{T_C}(\omega)\mid_{\omega=0}=\frac{\mathcal{K}T_f}{1-\mathcal{P}_{p_-}}, \quad \text{(B.5)}$$

and this completes the proof. ■

APPENDIX C
PROOF OF LEMMA 3

Proof: To derive π_i, the departure time of each data packet and all its replicas are considered. Particularly, at the m^{th} departure time, all $\mathcal{K}$ replicas related to the m^{th} transmission cycle are sent. Now, let $Q_m \in \{0, 1, 2, \ldots\}$ be the number of data packets in a typical IoT UE's buffer just after the m^{th} data packet departure.[10] Let A_{m+1} denote the number of packets arriving at the buffer during the $(m+1)^{th}$ transmission cycle. Then

$$Q_{m+1}=\begin{cases}Q_m+A_{m+1}, & \text{if } Q_m<p,\\ Q_m+A_{m+1}-p, & \text{if } Q_m\geq p.\end{cases} \quad \text{(C.1)}$$

Note that the arrival process is time-homogeneous and does not depend on transmission process. Moreover, Q_{m+1} depends only on A_{m+1} and Q_m, indicating that the stochastic process Q is a DTMC embedded at the end of transmission cycles. Hence, the stationary equations of π_i can be devised and solved, since the chain is irreducible and aperiodic. Specifically, by defining a_i as the probability of i data packets arriving during a transmission cycle, then

$$\pi_0=a_0\pi_0+a_0\pi_1+\cdots+a_0\pi_{p-1}+a_0\pi_p, \quad \text{(C.2.1)}$$
$$\pi_1=a_1\pi_0+a_1\pi_1+\cdots+a_1\pi_p+a_0\pi_{p+1},$$
$$\vdots \quad \text{(C.2.2)}$$

where the above equations can compactly be written as

$$\pi_j=a_j\pi_0+a_j\pi_1+\cdots+a_j\pi_p+a_{j-1}\pi_{p+1}+a_0\pi_{j+p}$$
$$=a_j\bar{\pi}_p+\sum_{i=p}^{j+p}\pi_i a_{j+p-i}, \quad \text{(C.3)}$$

in which $\bar{\pi}_p=\sum_{i=0}^{p-1}\pi_i$. Note that the stationary probabilities can recursively be obtained as

$$\pi_{j+p}=\frac{1}{a_0}\left(\pi_j-a_j\bar{\pi}_p-\sum_{i=p}^{j+p-1}\pi_i a_{j+p-i}\right). \quad \text{(C.4)}$$

[10]Note that each data departure consists of p data packets.

Also, a_i can be derived according to its definition, as

$$a_i=P\left(A_m=i\right)=\int_0^{\infty}P(A_m=i\mid T_C=t)f_{T_C}(t)dt$$
$$=\int_0^{\infty}\frac{(t\lambda_d)^i e^{-\lambda_p t}}{i!}f_{T_C}(t)dt, \quad \text{(C.5)}$$

which is obtained from the fact that the packet arrival process is Poisson with rate λ_d, as per **Remark 1**. Considering **Lemma 2**, then a_i (for $i=0, 1, \ldots$) can be determined as

$$a_i=\int_0^{\infty}\left[\frac{(t\lambda_d)^i e^{-\lambda_p t}}{i!}\right.$$
$$\left.\times\sum_{l=\mathcal{K}}^{\infty}\binom{l-1}{\mathcal{K}-1}\left(1-\mathcal{P}_{p_-}\right)^{\mathcal{K}}\left(\mathcal{P}_{p_-}\right)^{l-\mathcal{K}}\delta(t-lT_f)\right]dt$$
$$=\frac{1}{i!}\sum_{l=\mathcal{K}}^{\infty}\binom{l-1}{\mathcal{K}-1}\left(1-\mathcal{P}_{p_-}\right)^{\mathcal{K}}\left(\mathcal{P}_{p_-}\right)^{l-\mathcal{K}}$$
$$\times\int_0^{\infty}(t\lambda_d)^i e^{-\lambda_p t}\delta(t-lT_f)dt$$
$$=\frac{1}{i!}\sum_{l=\mathcal{K}}^{\infty}\binom{l-1}{\mathcal{K}-1}\left(1-\mathcal{P}_{p_-}\right)^{\mathcal{K}}\left(\mathcal{P}_{p_-}\right)^{l-\mathcal{K}}\left(lT_f\lambda_d\right)^i e^{-lT_f\lambda_d}$$
$$=\frac{\left(T_f\lambda_d\right)^i}{i!}\left(\frac{1-\mathcal{P}_{p_-}}{\mathcal{P}_{p_-}}\right)^{\mathcal{K}}\sum_{l=\mathcal{K}}^{\infty}\binom{l-1}{\mathcal{K}-1}l^i\left(\mathcal{P}_{p_-}e^{-T_f\lambda_d}\right)^l. \quad \text{(C.6)}$$

■

APPENDIX D
PROOF OF LEMMA 4

Proof: To obtain the first p steady-state probabilities π_i $(i=0, 1, \cdots, p-1)$, the z-operator is employed. Specifically, multiplying (C.4) by z^j and then summing over j yields

$$\sum_{j=0}^{\infty}\pi_j z^j=\sum_{j=0}^{\infty}\sum_{i=0}^{p-1}\pi_i a_j z^j+\sum_{j=0}^{\infty}\sum_{i=p}^{j+p}\pi_i a_{j+p-i}z^j. \quad \text{(D.1)}$$

Defining $\Lambda(z)\triangleq\sum_{j=0}^{\infty}\pi_j z^j$ and $\mathcal{A}(z)\triangleq\sum_{j=0}^{\infty}a_j z^j$, then (D.1) can be re-written as

$$\Lambda(z)=\sum_{i=0}^{p-1}\pi_i\mathcal{A}(z)+\sum_{j=0}^{\infty}\sum_{i=p}^{j+p}\pi_i a_{j+p-i}z^j$$
$$=\sum_{i=0}^{p-1}\pi_i\mathcal{A}(z)+\sum_{i=p}^{\infty}\sum_{j=i-p}^{j+p}\pi_i a_{j+p-i}z^j$$
$$=\sum_{i=0}^{p-1}\pi_i\mathcal{A}(z)+\sum_{i=p}^{\infty}\pi_i\left[z^{-(p-i)}\sum_{j=i-p}^{j+p}a_{j+p-i}z^{j+p-i}\right]$$
$$=\sum_{i=0}^{p-1}\pi_i\mathcal{A}(z)+\mathcal{A}(z)z^{-p}\sum_{i=p}^{\infty}\pi_i z^i$$
$$=\sum_{i=0}^{p-1}\pi_i\mathcal{A}(z)+\mathcal{A}(z)z^{-p}\left[\Lambda(z)-\sum_{i=0}^{p-1}\pi_i z^i\right]. \quad \text{(D.2)}$$

Finally, $\Lambda(z)$ is obtained as

$$\Lambda(z) = \frac{\mathcal{A}(z)\left(\bar{\pi}_p - z^{-p}\sum_{i=0}^{p-1}\pi_i z^i\right)}{1 - z^{-p}\mathcal{A}(z)}. \tag{D.3}$$

Note that $\Lambda(z)$ must not have any poles if it is to be stable. Hence, under the stability assumption and using Rouché theorem [52], and the fact that the arrival process is memoryless, the denominator of (D.3) (i.e. $1 - z^{-p}\mathcal{A}(z)$) has p distinct zeros, and these zeros must be canceled by the zeros of the numerator. Furthermore, $z = 1$ is one of the p denominator zeros, according to the property of moment generating function (i.e. $\mathcal{A}(1) = 1$). In turn, let the zeros of the denominator be denoted z_l (for $l = 1, \ldots, p$). Then, all π_i (for $i = 0, \ldots, p-1$) are determined by solving the zero-pole-cancellation set of equations, given by

$$\lim_{z\to 1}\Lambda(z) = 1, \tag{D.4a}$$

$$\mathcal{A}(z_l)\left(\bar{\pi}_p - z_l^{-p}\sum_{i=0}^{p-1}\pi_i z_l^i\right) = 0 \quad \text{for } l = 1, \ldots, p. \tag{D.4b}$$

Furthermore, $\mathcal{A}(z)$ can be derived as

$$\begin{aligned}\mathcal{A}(z) &= \sum_{i=0}^{\infty} a_i z^i = \sum_{i=0}^{\infty}\left[\int_0^{\infty}\frac{(t\lambda_d)^i}{i!}e^{-\lambda_p t} f_{T_C}(t)dt\right] z^i \\ &= \int_0^{\infty} e^{-\lambda_p t}\left(\sum_{i=0}^{\infty}\frac{(t\lambda_p z)^i}{i!}\right) f_{T_C}(t)dt \\ &= \int_0^{\infty} e^{-\lambda_p t} e^{\lambda_p z t} f_{T_C}(t)dt \\ &= \int_0^{\infty} e^{-(\lambda_d - \lambda_d z)t} f_{T_C}(t)dt \\ &= \mathcal{L}_{T_C}\left(\lambda_d(1-z)\right),\end{aligned} \tag{D.5}$$

in which $\mathcal{L}_{T_C}(.)$ is the Laplace transform of $f_{T_C}(t)$. Therefore, $\mathcal{A}(z)$ can be obtained using (B.3) as

$$\begin{aligned}\mathcal{A}(z) &= \mathcal{L}_{T_C}\left(\lambda_d(1-z)\right) = \Phi_{T_C}(\omega)\,|_{-j\omega=\lambda_d(1-z)} \\ &= \left(\frac{\left(1-\mathcal{P}_{p_-}\right)e^{\lambda_d(z-1)T_f}}{1-\mathcal{P}_{p_-}e^{\lambda_d(z-1)T_f}}\right)^{\mathcal{K}}.\end{aligned} \tag{D.6}$$

Since the numerator of $\mathcal{A}(z)$ in (D.6) is an exponential function, it includes no zeros, and hence $\mathcal{A}(z)$ can be removed from (D.4b). Finally, (D.4a) and (D.4b) can be simplified as

$$p(1-\bar{\pi}_p) = \Psi - \sum_{i=0}^{p-1} i\pi_i, \tag{D.7a}$$

$$\bar{\pi}_p - z_l^{-p}\sum_{i=0}^{p-1}\pi_i z_l^i = 0 \quad \text{for } l = 1, \ldots, p, \tag{D.7b}$$

where $\Psi \triangleq \frac{d}{dz}\mathcal{A}(z)\,|_{z=1}$ can be calculated from (D.6) as

$$\Psi = \frac{\mathcal{K}\lambda_d T_f}{1-\mathcal{P}_{p_-}}, \tag{D.8}$$

and the proof is now complete. ■

APPENDIX E
PROOF OF LEMMA 5

Proof: The average number of packets in a typical IoT UE's buffer can be derived using $\Lambda(z)$ in (D.3) as $\mathbb{E}[Q] = \frac{d}{dz}\Lambda(z)\,|_{z=1}$. Thus, the average packet waiting time $\mathbb{E}[\mathcal{W}]$ can be obtained by using Little's formulae, as given in (E.1) as shown at the bottom of the page [52]. Finally, the expression of μ_{T_L} in (10) is obtained by summing the expected value of transmission cycle in (6) and $\mathbb{E}[\mathcal{W}]$. ■

APPENDIX F
PROOF OF LEMMA 6

Proof: To derive $\mathcal{R}$, recall that for a data packet to be delivered successfully, at least one packet among its $\mathcal{K}$ replicas must be delivered without any collision or channel distortion.[11] Suppose the IoT UE of interest has at least p packets in its buffer and there are at least p idle RBs. Then, let P_e be the probability that a single packet experiences a collision and/or channel distortion. In turn, $\mathcal{R}$ is written as

$$\mathcal{R} = 1 - (P_e)^{\mathcal{K}}. \tag{F.1}$$

Let E_{NC} be the event that no collision (NC) occurs between the IoT UE of interest and the other IoT UEs. Also, let E_{NDE} be the event that the IoT UE experiences no decoding error (NDE) in its transmission. Since the aforementioned events are independent of each other, then P_e is expressed as

$$P_e = 1 - P(E_{NDE})P(E_{NC}), \tag{F.2}$$

where $P(E_{NDE})$ is obtained from (2) as

$$P(E_{NDE}) = 1 - \overline{\Upsilon}(\gamma, n_b, n_d). \tag{F.3}$$

[11] A typical data packet may encounter two types of errors; collision among IoT UEs selecting the same RBs, and channel decoding error due to channel distortion.

$$\begin{aligned}\mathbb{E}[\mathcal{W}] &= \frac{\mathbb{E}[Q]}{\lambda_d} \\ &= \frac{\Psi^2(\mathcal{K}+\mathcal{P}_{p^-}) + 2\mathcal{K}\Psi\left[p(\bar{\pi}_p - 1) - \sum_{i=0}^{p-1} i\pi_i\right] + \mathcal{K}p\,(1+p)\,(1-\bar{\pi}_p) - \mathcal{K}\sum_{i=0}^{p-1} i\,(i-1)\,\pi_i + 2\mathcal{K}p\sum_{i=0}^{p-1} i\pi_i}{2\mathcal{K}\lambda_p(p-\Psi)}\end{aligned} \tag{E.1}$$

To derive $P(E_{NC})$, two factors should be considered; the number of ready-to-transmit IoT UEs (i.e. the UEs that have at least p packets in their buffers), and the number of idle RBs. By denoting the former by N_p and the latter by N_{rb}, $P(E_{NC})$ can be written as

$$\begin{aligned} P(E_{NC}) &= \sum_{j=0}^{N-1} P(E_{NC} \,|\, N_p = j) P(N_p = j) \\ &= \sum_{j=0}^{N-1} P(E_{NC} \,|\, N_p = j) \binom{N-1}{j} (1-\bar{\pi}_p)^j \bar{\pi}_p^{N-1-j}. \end{aligned} \tag{F.4}$$

By further conditioning on N_{rb}, then

$$\begin{aligned} P(E_{NC}) = \sum_{j=0}^{N-1} \sum_{l=p}^{R} \Big[& P(E_{NC} \mid N_p = j, N_{rb} = l) \\ & \times P(N_{rb} = l \mid N_p = j) \binom{N-1}{j} (1-\bar{\pi}_p)^j \bar{\pi}_p^{N-1-j} \Big], \end{aligned} \tag{F.5}$$

where it should be noted that N_p and N_{rb} are independent. Moreover, all RBs are also independent of each other. Hence,

$$\begin{aligned} P(N_{rb} = l \mid N_p = j) &= P(N_{rb} = l) \\ &= \binom{R}{l} \Pi_0^l (1-\Pi_0)^{R-l}. \end{aligned} \tag{F.6}$$

Also, $P(E_{NC} \mid N_p = j, N_{rb} = l)$ in (F.5) can be written as

$$P(E_{NC} \mid N_p = j, N_{rb} = l) = \left(\frac{\binom{l-p}{p}}{\binom{l}{p}} \right)^j. \tag{F.7}$$

Note that when $N_p \neq 0$, there must be at least $2p$ idle RBs to avoid any collision according to *Pigeonhole principle* (i.e. $N_{rb} \geq 2p$) [53]. For $N_p = 0$, no collision happens in the underlying transmission. Thus, from (F.5)-(F.7), $P(E_{NC})$ is obtained as

$$\begin{aligned} P(E_{NC}) = \sum_{j=1}^{N-1} \sum_{l=2p}^{R} & \left(\frac{\binom{l-p}{p}(1-\bar{\pi}_p)}{\binom{l}{p}} \right)^j \binom{R}{l} \Pi_0^l (1-\Pi_0)^{R-l} \\ & + \sum_{l=p}^{R} \binom{R}{l} \Pi_0^l (1-\Pi_0)^{R-l}. \end{aligned} \tag{F.8}$$

Finally, substituting (F.3) and (F.8) into (F.2) yields P_e, which is used to obtain the expression of $\mathcal{R}$ in (11) via (F.1). ∎

APPENDIX G
PROOF OF LEMMA 7

Proof: The energy-efficiency is defined as

$$\eta_e \triangleq \frac{\mathbb{E}\left[R_{\mathit{eff}}\right]}{\mathbb{E}\left[\mathcal{E}^c\right]}, \tag{G.1}$$

where R_{eff} is the effective rate and $\mathcal{E}^c$ is the consumed energy in a transmission cycle. Thus, $\mathbb{E}\left[R_{\mathit{eff}}\right]$ is written as

$$\mathbb{E}\left[R_{\mathit{eff}}\right] = \frac{\mathbb{E}[B_{\mathit{eff}}]}{\mathbb{E}[T_C]}, \tag{G.2}$$

where $\mathbb{E}[B_{\mathit{eff}}]$ is the average transferred bits in a transmission cycle, and $\mathbb{E}[T_C]$ is the average transmission cycle. Conditioning over all frame types, $\mathbb{E}[B_{\mathit{eff}}]$ is obtained as

$$\begin{aligned} \mathbb{E}[B_{\mathit{eff}}] &= \sum_{i=0}^{\infty} \mathbb{E}[B_{\mathit{eff}} \mid \mathcal{T}_i] \pi_i = \sum_{i=p}^{\infty} \mathbb{E}[B_{\mathit{eff}} \mid \mathcal{T}_i] \pi_i \\ &= \sum_{i=p}^{\infty} p n_d \mathcal{R} \pi_i = p n_d \mathcal{R} (1-\bar{\pi}_p). \end{aligned} \tag{G.3}$$

Note that the summation over $i = 0$ to $i = p-1$ is zero, since at least p packets should exist in the IoT UE's buffer to start transmission. Moreover, **Lemma 2** provides $\mathbb{E}[T_C]$ in (6). To derive the average amount of consumed energy in a typical transmission cycle, recall that each transmission cycle consists of $\mathcal{K}$ attempts for sending a typical packet group (i.e. p packets) in a TTI. Also, note that each packet group has a transmission delay distribution $f_{T_D}(t)$, as derived in **Lemma 1**. Thus, by denoting $\mathcal{K}\mathbb{E}\left[\mathcal{E}_{\mathcal{T}}^c\right]$ as the average amount of consumed energy for transmission of a typical packet group at one attempt, $\mathbb{E}\left[\mathcal{E}^c\right]$ is obtained as

$$\begin{aligned} &\mathbb{E}\left[\mathcal{E}^c\right] \\ &= \mathcal{K}\mathbb{E}\left[\mathcal{E}_{\mathcal{T}}^c\right] \\ &= \mathcal{K} \sum_{i=p}^{\infty} \mathbb{E}\left[\mathcal{E}_{\mathcal{T}}^c \mid \mathcal{T}_i\right] \pi_i \\ &= \mathcal{K}\mathbb{E}\left[\mathcal{E}_{\mathcal{T}}^c \mid \mathcal{T}_i\right] (1-\bar{\pi}_p) \\ &= \mathcal{K}(1-\bar{\pi}_p) \int_0^{\infty} \mathbb{E}\left[\mathcal{E}^c \mid \mathcal{T}_i, D = t\right] f_{T_D|\mathcal{T}_i}(t) dt \\ &= \mathcal{K}(1-\bar{\pi}_p) \sum_{j=1}^{\infty} \mathbb{E}\left[\mathcal{E}^c \mid T_D = jT_f\right] \left(\mathcal{P}_{p_-}\right)^{j-1} \left(1-\mathcal{P}_{p_-}\right). \end{aligned} \tag{G.4}$$

Note that $f_{T_D|\mathcal{T}_i}(t) = f_{T_D}(t)$, since the transmission delay does not depend on the TTI type. Further, note that a if the IoT UE has j attempts to transmit in a typical TTI, on the last attempt, the packets in the TTI are sent and the IoT node has not found at least p idle RBs in its first $j-1$ attempts. Hence, $\mathbb{E}\left[\mathcal{E}^c \mid T_D = jT_f\right] = \mathbb{P}_t T_f + (j-1)\mathbb{P}_c T_f$. Finally,

$$\begin{aligned} \mathbb{E}\left[\mathcal{E}^c\right] &= \mathcal{K}(1-\bar{\pi}_p)\left(1-\mathcal{P}_{p_-}\right) \\ &\quad \times \sum_{j=1}^{\infty} \left[\left(\mathbb{P}_t T_f + (j-1)\mathbb{P}_c T_f \right) \left(\mathcal{P}_{p_-}\right)^{j-1} \right] \\ &= \mathcal{K}(1-\bar{\pi}_p) \left(\mathbb{P}_t T_f + \frac{\mathbb{P}_c T_f \mathcal{P}_{p_-}}{1-\mathcal{P}_{p_-}} \right). \end{aligned} \tag{G.5}$$

Substituting (G.3) and (6) into (G.2), and then (G.2) and (G.5) into (G.1) yields η_e in (14). ∎

APPENDIX H
PROOF OF LEMMA 8

Proof: By using conditional expectation, $\mathbb{E}[\mathcal{E}_m^c]$ is expressed as

$$\mathbb{E}[\mathcal{E}_m^c] = \sum_{i=0}^{\infty} \mathbb{E}[\mathcal{E}_m^c \mid \mathcal{T}_i]\pi_i = \sum_{i=p}^{\infty} \mathbb{E}[\mathcal{E}_m^c \mid \mathcal{T}_i]\pi_i. \tag{H.1}$$

Note that the IoT UE does not transmit data if there are less than p packets in its buffer, and hence, it experiences no energy consumption in that case. Furthermore, the average energy consumption in a frame depends on whether transmission occurs in that frame or the IoT UE waits for the next frame, which means it could not find the required p idle RBs. Recall that N_{rb} is a random variable resembling the number of idle RBs found by the IoT UE at the beginning of the underlying frame, then $\mathbb{E}[\mathcal{E}_m^c]$ is derived as

$$\begin{aligned}\mathbb{E}[\mathcal{E}_m^c] &= \sum_{i=p}^{\infty}\sum_{l=0}^{r} \mathbb{E}[\mathcal{E}_m^c \mid \mathcal{T}_i, N_{rb}=l]\pi_i P(N_{rb}=l) \\ &= \sum_{i=p}^{\infty}\sum_{l=0}^{p-1} \mathbb{E}[\mathcal{E}_m^c \mid \mathcal{T}_i, N_{rb}=l]\pi_i P(N_{rb}=l) \\ &\quad + \sum_{i=p}^{\infty}\sum_{l=p}^{R} \mathbb{E}[\mathcal{E}_m^c \mid \mathcal{T}_i, N_{rb}=l]\pi_i P(N_{rb}=l). \end{aligned} \tag{H.2}$$

If the IoT UE waits for the next frame (or TTI) to transmit its data, its energy consumption will be $\mathbb{P}_c T_f$. If it is able to transmit data, it will consume $\mathbb{P}_t T_f$ amount of energy. Thus, the expected amount of consumed energy is determined as

$$\begin{aligned}&\mathbb{E}[\mathcal{E}_m^c] \\ &= \sum_{i=p}^{\infty}\sum_{l=0}^{p-1} \mathbb{P}_c T_f \pi_i P(N_{rb}=l) + \sum_{i=p}^{\infty}\sum_{l=p}^{R} \mathbb{P}_t T_f \pi_i P(N_{rb}=l) \\ &= \mathbb{P}_c T_f \sum_{i=p}^{\infty}\pi_i \sum_{l=0}^{p-1} P(N_{rb}=l) + \mathbb{P}_t T_f \sum_{i=p}^{\infty}\pi_i \sum_{l=p}^{R} P(N_{rb}=l) \\ &= \mathbb{P}_c T_f (1-\bar{\pi}_p)\mathcal{P}_{p_-} + \mathbb{P}_t T_f (1-\bar{\pi}_p)(1-\mathcal{P}_{p_-}) \\ &= (1-\bar{\pi}_p)\Big((\mathbb{P}_c - \mathbb{P}_t)\mathcal{P}_{p_-} + \mathbb{P}_t\Big)T_f. \end{aligned} \tag{H.3}$$

Finally, the average harvested energy in a frame is $\lambda_h T_f$ and then the energy-causality constraint is derived as in (15). ∎

REFERENCES

[1] G. Hampel, C. Li, and J. Li, "5G ultra-reliable low-latency communications in factory automation leveraging licensed and unlicensed bands," *IEEE Commun. Mag.*, vol. 57, no. 5, pp. 117–123, May 2019.

[2] Z. Ma, M. Xiao, Y. Xiao, Z. Pang, H. V. Poor, and B. Vucetic, "High-reliability and low-latency wireless communication for Internet of Things: Challenges, fundamentals, and enabling technologies," *IEEE Internet Things J.*, vol. 6, no. 5, pp. 7946–7970, Oct. 2019.

[3] M. A. Siddiqi, H. Yu, and J. Joung, "5G ultra-reliable low-latency communication implementation challenges and operational issues with IoT devices," *Electronics*, vol. 8, no. 9, p. 981, Sep. 2019. [Online]. Available: https://www.mdpi.com/2079-9292/8/9/981

[4] S. Haykin, "Cognitive radio: Brain-empowered wireless communications," *IEEE J. Sel. Areas Commun.*, vol. 23, no. 2, pp. 201–220, Feb. 2005.

[5] M.-L. Ku, W. Li, Y. Chen, and K. J. R. Liu, "Advances in energy harvesting communications: Past, present, and future challenges," *IEEE Commun. Surveys Tuts.*, vol. 18, no. 2, pp. 1384–1412, 2nd Quart., 2016.

[6] M. Shirvanimoghaddam, M. S. Mohammadi, R. Abbas, A. Minja, C. Yue, B. Matuz, G. Han, Z. Lin, W. Liu, Y. Li, S. Johnson, and B. Vucetic, "Short block-length codes for ultra-reliable low latency communications," *IEEE Commun. Mag.*, vol. 57, no. 2, pp. 130–137, Feb. 2019.

[7] P. Popovski, C. Stefanovic, J. J. Nielsen, E. de Carvalho, M. Angjelichinoski, K. F. Trillingsgaard, and A.-S. Bana, "Wireless access in ultra-reliable low-latency communication (URLLC)," *IEEE Trans. Commun.*, vol. 67, no. 8, pp. 5783–5801, Aug. 2019.

[8] G. J. Sutton, J. Zeng, R. P. Liu, W. Ni, D. N. Nguyen, B. A. Jayawickrama, X. Huang, M. Abolhasan, Z. Zhang, E. Dutkiewicz, and T. Lv, "Enabling technologies for ultra-reliable and low latency communications: From PHY and MAC layer perspectives," *IEEE Commun. Surveys Tuts.*, vol. 21, no. 3, pp. 2488–2524, 3rd Quart., 2019.

[9] H. Ren, C. Pan, Y. Deng, M. Elkashlan, and A. Nallanathan, "Joint power and blocklength optimization for URLLC in a factory automation scenario," *IEEE Trans. Wireless Commun.*, vol. 19, no. 3, pp. 1786–1801, Mar. 2020.

[10] C. She, C. Yang, and T. Q. S. Quek, "Cross-layer optimization for ultra-reliable and low-latency radio access networks," *IEEE Trans. Wireless Commun.*, vol. 17, no. 1, pp. 127–141, Jan. 2018.

[11] J. Khan and L. Jacob, "Availability maximization framework for CoMP enabled URLLC with short packets," *IEEE Netw. Lett.*, vol. 2, no. 1, pp. 1–4, Mar. 2020.

[12] A. Anand and G. de Veciana, "Resource allocation and HARQ optimization for URLLC traffic in 5G wireless networks," *IEEE J. Sel. Areas Commun.*, vol. 36, no. 11, pp. 2411–2421, Nov. 2018.

[13] F. Librino and P. Santi, "Resource allocation and sharing in URLLC for IoT applications using shareability graphs," *IEEE Internet Things J.*, vol. 7, no. 10, pp. 10511–10526, Oct. 2020.

[14] A. Karimi, K. I. Pedersen, N. H. Mahmood, J. Steiner, and P. Mogensen, "5G centralized multi-cell scheduling for URLLC: Algorithms and system-level performance," *IEEE Access*, vol. 6, pp. 72253–72262, 2018.

[15] A. Avranas, M. Kountouris, and P. Ciblat, "Energy-latency tradeoff in ultra-reliable low-latency communication with retransmissions," *IEEE J. Sel. Areas Commun.*, vol. 36, no. 11, pp. 2475–2485, Nov. 2018.

[16] P. Popovski, K. F. Trillingsgaard, O. Simeone, and G. Durisi, "5G wireless network slicing for eMBB, URLLC, and mMTC: A communication-theoretic view," *IEEE Access*, vol. 6, pp. 55765–55779, Sep. 2018.

[17] G. Pocovi, K. I. Pedersen, and P. Mogensen, "Joint link adaptation and scheduling for 5G ultra-reliable low-latency communications," *IEEE Access*, vol. 6, pp. 28912–28922, May 2018.

[18] Y. K. Tun, D. H. Kim, M. Alsenwi, N. H. Tran, Z. Han, and C. S. Hong, "Energy efficient communication and computation resource slicing for eMBB and URLLC coexistence in 5G and beyond," *IEEE Access*, vol. 8, pp. 136024–136035, Jul. 2020.

[19] M. R. Amini and M. W. Baidas, "Random-access NOMA in URLL energy-harvesting IoT networks with short packet and diversity transmissions," *IEEE Access*, vol. 8, pp. 220734–220754, Dec. 2020.

[20] M. R. Amini and M. W. Baidas, "Performance analysis of URLL random-access NOMA-enabled IoT networks with short packet and diversity transmissions," in *Proc. Int. Conf. Commun., Signal Process., Appl. (ICCSPA)*, Mar. 2021, pp. 1–6.

[21] Q. Huang, X. Xie, H. Tang, T. Hong, M. Kadoch, K. K. Nguyen, and M. Cheriet, "Machine-learning-based cognitive spectrum assignment for 5G URLLC applications," *IEEE Netw.*, vol. 33, no. 4, pp. 30–35, Jul. 2019.

[22] W. Yu, A. U. Quddus, S. Vahid, and R. Tafazolli, "Opportunistic spectrum access in support of ultra-reliable and low latency communications," in *Proc. IEEE GLOBECOM Workshops (GC Wkshps)*, Dec. 2018, pp. 1–7.

[23] J. Lin, W. Yu, N. Zhang, X. Yang, H. Zhang, and W. Zhao, "A survey on Internet of Things: Architecture, enabling technologies, security and privacy, and applications," *IEEE Internet Things J.*, vol. 4, no. 5, pp. 1125–1142, Oct. 2017.

[24] B. Moon, "Dynamic spectrum access for Internet of Things service in cognitive radio-enabled LPWANs," *Sensors*, vol. 17, no. 12, pp. 1–21, 2017.

[25] A. O. Ercan, M. O. Sunay, and I. F. Akyildiz, "RF energy harvesting and transfer for spectrum sharing cellular IoT communications in 5G systems," *IEEE Trans. Mobile Comput.*, vol. 17, no. 7, pp. 1680–1694, Jul. 2018.

[26] T. Li, J. Yuan, and M. Torlak, "Network throughput optimization for random access narrowband cognitive radio Internet of Things (NB-CR-IoT)," *IEEE Internet Things J.*, vol. 5, no. 3, pp. 1436–1448, Jun. 2018.
[27] R. M. Sandoval, A.-J. Garcia-Sanchez, J. Garcia-Haro, and T. M. Chen, "Optimal policy derivation for transmission duty-cycle constrained LPWAN," *IEEE Internet Things J.*, vol. 5, no. 4, pp. 3114–3125, Aug. 2018.
[28] P. Karunakaran and W. Gerstacker, "A reference signal based GLRT for simultaneous sensing and reception in cognitive LTE-A systems," in *Proc. IEEE Wireless Commun. Netw. Conf.*, Apr. 2016, pp. 1–6.
[29] V. Gupta, S. K. Devar, N. H. Kumar, and K. P. Bagadi, "Modelling of IoT traffic and its impact on LoRaWAN," in *Proc. IEEE Global Commun. Conf. (GLOBECOM)*, Dec. 2017, pp. 1–6.
[30] T. Hoßfeld, F. Metzger, and P. E. Heegaard, "Traffic modeling for aggregated periodic IoT data," in *Proc. 21st Conf. Innov. Clouds, Internet Netw. Workshops (ICIN)*, Feb. 2018, pp. 1–8.
[31] Y. Polyanskiy, H. V. Poor, and S. Verdu, "Channel coding rate in the finite blocklength regime," *IEEE Trans. Inf. Theory*, vol. 56, no. 5, pp. 2307–2359, May 2010.
[32] W. Gabran, C.-H. Liu, P. Pawelczak, and D. Cabric, "Primary user traffic estimation for dynamic spectrum access," *IEEE J. Sel. Areas Commun.*, vol. 31, no. 3, pp. 544–558, Mar. 2013.
[33] Z. Shi, K. C. Teh, and K. H. Li, "Joint design of sensing and transmission in energy-efficient cognitive radio systems over fading channels," *IET Commun.*, vol. 7, no. 6, pp. 577–584, Apr. 2013.
[34] Y. Saleem and M. H. Rehmani, "Primary radio user activity models for cognitive radio networks: A survey," *J. Netw. Comput. Appl.*, vol. 43, pp. 1–16, Aug. 2014.
[35] S. M. Ross, *Introduction to Probability Models*, 10th ed. Amsterdam, The Netherlands: Elsevier, 2010.
[36] G. Han, J.-K. Zhang, and X. Mu, "Joint optimization of energy harvesting and detection threshold for energy harvesting cognitive radio networks," *IEEE Access*, vol. 4, pp. 7212–7222, 2016.
[37] S. Park and D. Hong, "Achievable throughput of energy harvesting cognitive radio networks," *IEEE Trans. Wireless Commun.*, vol. 13, no. 2, pp. 1010–1022, Feb. 2014.
[38] Y. Gao, H. He, Z. Deng, and X. Zhang, "Cognitive radio network with energy-harvesting based on primary and secondary user signals," *IEEE Access*, vol. 6, pp. 9081–9090, 2018.
[39] O. B. Akan, O. Cetinkaya, C. Koca, and M. Ozger, "Internet of hybrid energy harvesting things," *IEEE Internet Things J.*, vol. 5, no. 2, pp. 736–746, Apr. 2018.
[40] *LTE; Evolved Universal Terrestrial Radio Access (E-UTRA); Radio Frequency (RF) System Scenarios*, document ETSI TR 136 942 V13.0.0, 3rd Generation Partnership Project, 2016. [Online]. Available: https://www.portal.3gpp.org
[41] *Technical Specification Group Services and System Aspects; Service Requirements for the 5G System; Stage 1*, document TS 22.261 V17.3.0, 3GPP, 2020. [Online]. Available: https://www.portal.3gpp.org
[42] P. Popovski, C. Stefanović, J. J. Nielsen, E. de Carvalho, M. Angjelichinoski, K. F. Trillingsgaard, and A.-S. Bana, "Wireless access in ultra-reliable low-latency communication (URLLC)," *IEEE Trans. Commun.*, vol. 67, no. 8, pp. 5783–5801, Aug. 2019.
[43] *Telecommunication Standardization Sector of ITU*, document Rec. ITU-T E.800, ITU, Jul. 2009. [Online]. Available: http://www.itu.int/rec/T-REC-E.800-200809-I/en
[44] *Technical Specification Group Radio Access Network; Study on NR Industrial Internet of Things (IoT)*, document TR 38.825 V16.0.0, 3GPP, 2019. [Online]. Available: http://www.portal.3gpp.org
[45] G. L. Nemhauser, *Integer and Combinatorial Optimization*. Hoboken, NJ, USA: Wiley, 1988.
[46] M. Schlueter, "MIDACO software performance on interplanetary trajectory benchmarks," *Adv. Space Res.*, vol. 54, no. 4, pp. 744–754, Aug. 2014.
[47] MIDACO-Solver. *Mixed Integer Distributed Ant Colony Optimization*. Accessed: Apr. 13, 2021. [Online]. Available: http://www.midaco-solver.com
[48] C. She, C. Sun, Z. Gu, Y. Li, C. Yang, H. V. Poor, and B. Vucetic, "A tutorial on ultrareliable and low-latency communications in 6G: Integrating domain knowledge into deep learning," *Proc. IEEE*, vol. 109, no. 3, pp. 204–246, Mar. 2021.
[49] Z. Qin, H. Ye, G. Y. Li, and B.-H.-F. Juang, "Deep learning in physical layer communications," *IEEE Wireless Commun.*, vol. 26, no. 2, pp. 93–99, Apr. 2019.
[50] Z. Hou, C. She, Y. Li, T. Q. S. Quek, and B. Vucetic, "Burstiness-aware bandwidth reservation for ultra-reliable and low-latency communications in tactile Internet," *IEEE J. Sel. Areas Commun.*, vol. 36, no. 11, pp. 2401–2410, Nov. 2018.
[51] A. Leon-Garcia, *Probability, Statistics, and Random Processes for Electrical Engineering*. London, U.K.: Pearson, 2008.
[52] G. Giambene, *Queuing Theory and Telecommunications: Networks and Applications*. New York, NY, USA: Springer, 2014.
[53] S. Jukna, *The Pigeonhole Principle*. Berlin, Germany: Springer, 2011, pp. 53–75.

MOHAMMAD REZA AMINI (Senior Member, IEEE) received the B.Eng. degree in electrical and communication system engineering from the Isfahan University of Technology (IUT), Isfahan, Iran, the M.Sc. degree in electrical and communication system engineering from the Malek-Ashtar University of Technology, Iran, and the Ph.D. degree in telecommunications from IUT, in 2018. He is currently an Assistant Professor with the Department of Electrical Engineering, Islamic Azad University, Borujerd Branch, Iran. He is also an Inspector of Iran's Standard Institute and accepted in National Foundation of Elites. His research interests include cognitive radio networks, system implementation, and green and energy-harvesting networks. He was a recipient of the Outstanding Teaching and Outstanding Researcher Award, in 2012, 2016, 2017, and 2018.

MOHAMMED W. BAIDAS (Senior Member, IEEE) received the B.Eng. degree (Hons.) in communication systems engineering from The University of Manchester, Manchester, U.K., in 2005, the M.Sc. degree (Hons.) in wireless communications engineering from the University of Leeds, Leeds, U.K., in 2006, the M.S. degree in electrical engineering from the University of Maryland, College Park, MD, USA, in 2009, and the Ph.D. degree in electrical engineering from Virginia Tech, Blacksburg, VA, USA, in 2012. He was a Visiting Researcher with the University of Manchester, in the academic years of 2015–2016 and 2018–2019. He is currently an Associate Professor with the Department of Electrical Engineering, Kuwait University, Kuwait, where he has been with the faculty, since May 2012. He is also a frequent reviewer for several IEEE journals and international journals and conferences, with over 80 publications. His research interests include resource allocation and management in cognitive radio systems, game theory, cooperative communications and networking, and green and energy-harvesting networks. He also serves as a technical program committee member for various IEEE and international conferences. He was a recipient of the Outstanding Teaching Award of Kuwait University, for the academic year of 2017–2018.